

# Fat-Water Separation with High Temporal and Spatial Resolution for Abdominal MRI during Free Breathing

Riad S. Ababneh<sup>1</sup>, Thomas Benkert<sup>2</sup>, Felix A. Breuer<sup>2</sup>

## Abstract

**Objective:** To separate the fat and water contents in the abdomen during free breathing at high temporal and high spatial resolution by employing radial sampling with a golden angle increment.

**Materials and Methods:** A radial fast imaging with steady-state free precession (TrueFISP) sequence was used and modified to allow for different echo times (TEs) for subsequent radial projections for fat-water separation. The k-space-weighted image contrast (KWIC) radial filtering technique was applied to enable high temporal as well as high spatial resolution. Finally, principal component analysis (PCA) was performed along the dynamic image series in order to reduce image streaking and enhance the signal-to-noise ratio (SNR).

**Results:** The approach was combined with the KWIC filter and provided good fat-water separation with a robust high temporal (~100 ms) and high spatial resolution. Results for the abdomen with free breathing are presented.

**Conclusion:** Good separation of fat and water signals was achieved using the radial TrueFISP sequence during free breathing

**Keywords:** Fat-water separation, TrueFISP, KWIC, Dynamic imaging, Free breathing.

(J Med J 2017; Vol. 51(3):131-139)

Received

April 19, 2016

Accepted

July 5, 2017

## Introduction

Fat and water separation in dynamic MRI plays a critical role in many applications, such as breast imaging, where bright fat signals can obscure breast cancer lesions, as well as arrhythmogenic right-ventricular dysplasia (ARVD), characterized by fat infiltrations into

the right ventricular wall<sup>(1-3)</sup> and abdominal imaging<sup>(4)</sup>. The separation takes advantage of the resonance frequency difference between fat and water signals, which make it possible to generate images where these two types of tissues are separated<sup>(5-10)</sup>. For abdominal imaging applications, several MRI techniques have been used for fat-water separation. These include the

1. Assistant Professor of Health Physics, Physics Department, Yarmouk University, Irbid 21163, Jordan.

2. Research Center Magnetic Resonance Bavaria, Würzburg, Germany.

\* Correspondence should be addressed to:

E-mail: riada@yu.edu.jo

Assistant Professor of Health Physics, Physics Department, Yarmouk University, Irbid 21163, Jordan.

E-mail: riada@yu.edu.jo

Dixon method<sup>(5-6)</sup>, direct phase encoding (DPE)<sup>(7)</sup>, and iterative decomposition of water and fat with echo asymmetry and least-square estimation (IDEAL)<sup>(8-9)</sup>. Robust fat-water separation with dynamic objects remains a challenge, especially in the presence of respiratory motion when imaging the abdomen. Respiratory motion can lead to significant image quality deterioration and inaccurate measurements such as ghosting and blurring artifacts in the reconstructed data. Free breathing abdominal imaging could be combined with the methods proposed in this work to avoid respiratory motion artifacts, while continuing to provide high temporal and high spatial resolution<sup>(11-12)</sup>. The applied strategies for fat-water separation are required at least two images for the separation to be performed, therefore, it's difficult to achieve good temporal resolution in dynamic imaging<sup>(5-10)</sup>. In contrast, Ababneh et al.<sup>(13)</sup> succeeded in separating fat and water signals in dynamic MRI and provided improved temporal resolution by the combined three-point Dixon method for fat-water separation and unaliasing by Fourier-encoding the overlaps using the temporal dimension (UNFOLD)<sup>(14-16)</sup>. This method involves an assumption that fat signals are not very dynamic. Even when fat signals prove to be quite dynamic, suppressing their low temporal frequency content is expected to lead to significant overall suppression. This method provided a unique combination of imaging speed, high signal-to-noise ratio (SNR) and high contrast between the myocardium and blood pool. In this work, the previously published method<sup>(13)</sup> was used with free breathing to achieve fat-water separation in the abdomen and combined with k-space-weighted image contrast (KWIC) filtering and principal component analysis (PCA)<sup>(17-18)</sup>. Therefore, a regular 2D radial TrueFISP sequence was modified to allow TE to vary from projection to

the next. TE was adjusted here in a predetermined manner, to force fat signals to behave in a peculiar and readily recognizable fashion over time. TrueFISP (or balanced steady state free precession bSSFP) provides a unique combination of imaging speed, high signal-to-noise ratio (SNR), and high contrast between the myocardium and blood pool. By using temporal processing, the temporal variations imposed the fat signals to behave in a different manner to be recognized, therefore, the fat signals could be separated from water signals.

Radial MRI has gained increasing attention in dynamic imaging and has been used in many applications such as cardiac imaging<sup>(19-22)</sup> and abdominal imaging<sup>(23-24)</sup>. Radial MRI has a higher sampling density for the central k-space and higher spatial and temporal resolution, and is insensitive to object motion during data acquisition<sup>(25-26)</sup>. Therefore, radial MRI was incorporated into this work.

The k-space-weighted image contrast (KWIC) filtering technique is useful in many applications, such as dynamic contrast-enhanced (DCE)-MRI<sup>(27)</sup>, cardiac imaging and applications involving object motion. The KWIC filter improves the acquired data<sup>(17-18)</sup>. Principal component analysis (PCA) was used to analyze the dynamic data by decomposing the events from an observation matrix<sup>(28)</sup>, and indicated the components that contributed to image streaking artifacts<sup>(17)</sup>. This work aims to separate the fat and water contents in the abdomen during free breathing with high spatial resolution and high temporal resolution. These goals were achieved by integrating the fat-water separation method in<sup>(13)</sup> with KWIC-filtered 2D radial TrueFISP sequence, the (PCA) technique will also be used to reduce image streaking artifacts and enhance the (SNR) during free breathing imaging. The results were obtained in vivo at 3.0T for the abdomen.

## Materials and methods

Five healthy volunteers participated in the study following the guidelines of the local institutional review board including written informed consent. The method aimed at significantly increasing the temporal resolution of a series of fat and water images by maintaining high in-plane resolution. This approach will be applicable for abdominal imaging with artifact-free fat-water separation in the abdomen during free breathing. In this approach, we acquire subsequent projections with different TEs (2001 projections). Since in radial imaging the center of k-space is acquired with each radial line and the golden angle projection order provides homogenous k-space coverage at any time, our sequence allows to reconstruct images at any point in time in a sliding window approach. Since the contrast of the images is dominated by the center of k-space only data from a few projections around the time point to be reconstructed are used in the center of k-space. This procedure is known as KWIC filtering Fig.1. In the case of motion between subsequent images fat-water separation will fail as the reconstruction is based on a pixel by pixel basis. In contrast, by acquiring subsequent projections with different TEs the presented approach is much more robust against motion and provides artifact-free fat-water separation. Figure 1, shows the principle of the KWIC filter process. The method was implemented at 3.0T using the modified 2D radial TrueFISP sequence. This work uses the 2D radial TrueFISP sequence, characterized by a train of alternating excitation pulses ( $\pm\alpha$ ), separated by a constant time interval (repetition time; TR). It starts with a number of RF pulses to hasten the set-up of steady state magnetization. In this sequence the gradients are balanced, i.e., the three gradient waveforms integrated over a TR interval give zero, for a null zeroth moment. In

this sequence, the transverse magnetization is fully refocused within each TR interval<sup>(13)</sup>. To achieve fat and water separation, the 2D radial TrueFISP pulse sequence was modified to enable TE changes from one radial projection to the next, as demonstrated in Fig. 2a. at constant TR<sup>(13)</sup>. The four TEs were periodically repeated following a radial golden angle projection order  $\phi_{GR} = 111.246$ . A large number of images with different contrast were generated using the KWIC technique for each data set. In this technique (initially proposed by Song<sup>(17-18)</sup>), a reconstruction window starts with number of projections (eight projections in this work for the first keyhole ring) and increases according to the Fibonacci series<sup>(17)</sup>. The number of projections contributing to each keyhole ring should match a Fibonacci number to achieve optimal k-space coverage. A density compensation function (DCF) is used to filter each projection to make sure that the image intensity and contrast is the average of all contributing views<sup>(29)</sup>. The images were filtered using the KWIC filter, then reconstructed using the non-uniform fast Fourier transform (NUFFT) from the image reconstruction toolbox by Fessler et al.<sup>(30)</sup>. In total, 2001 projections were acquired at four different TEs, and 631 KWIC-filtered projections were used to reconstruct four images at different TEs at 21 different time points. Experiments were performed on a 3.0T scanner (Magnetom Skyra, Siemens Healthcare, Erlangen, Germany) using a 32-spinal coil positioned about the mid portion of the body and body array. The imaging parameters were: TR = 4.0 ms, (TE<sub>1</sub> = 1.6 ms, TE<sub>2</sub> = 2.4 ms, TE<sub>3</sub> = 1.6 ms, TE<sub>4</sub> = 2 ms), matrix size = 256 x 256, flip angle = 40°, FOV= 400x400 mm<sup>2</sup>, slice thickness = 5 mm, total scan time = 34 sec and the total reconstruction time 15-20 min. PCA was applied along the time series and principal components with small eigenvalues were

removed. All acquired data was reconstructed offline using a Matlab software package (Math Works, Natick, MA). Finally, fat-water separation according to Ref. 13 was applied frame by frame.

**Results**

The results of the modified sequence and in vivo studies are shown in Fig. 1, Fig. 2, Fig. 3, Fig. 4 and Fig. 5. Fig. 2 describes the modified sequence, where TE changes from projection to projection (Fig. 2b). As shown in Fig. 2a, TE(t) takes on the successive values of TEs, where  $TE_1 = TE_0$ ,  $TE_2 = TE_0 + 2\Delta TE$ ,  $TE_3 = TE_0$ , and

$TE_4 = TE_0 + \Delta TE$ .  $\Delta TE$  is the echo time increment and  $TE_0$  is the smallest possible echo time allowed by the unmodified sequence. The echo time increment  $\Delta TE$  was kept extremely short in this work ( $\sim 400 \mu s$ ). In comparison, in the original description of the three-point Dixon method<sup>(5)</sup>,  $\Delta TE$  would be the value required for an 180° offset between the fat and water signals. This choice of a short 400  $\mu s$   $\Delta TE$  stems from the need to keep TE and TR short in a TrueFISP sequence (Short TR and TE are required to prevent signal loss and artifacts in the presence of field inhomogeneities).

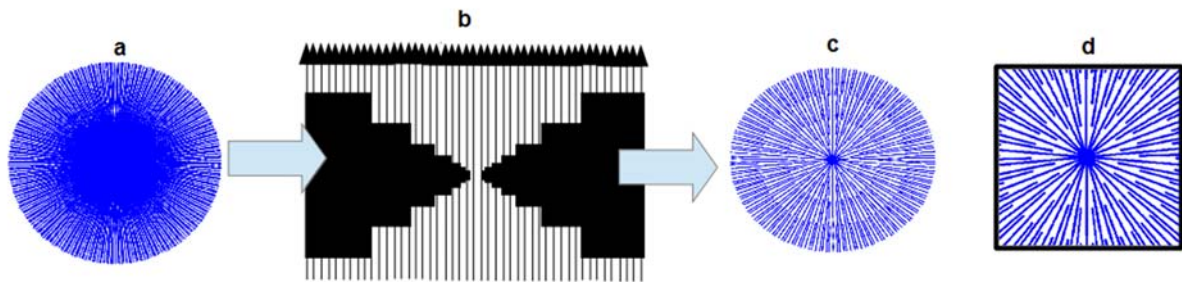


**Figure 1: Schematic of the radial acquisition following a golden angle projection (a) and the corresponding KWIC filter procedure (b). The KWIC filter results in a k-space (filtered projection within the reconstruction window). (c) and (d) where only a few projections around the time point to reconstruct are used in the center of k-space allowing for high temporal resolution. Projections further away are used to fill the k-space periphery to provide sufficient spatial resolution**

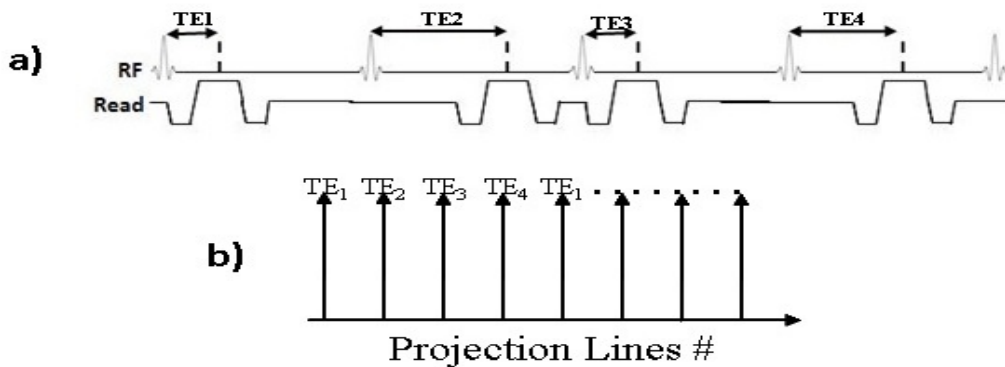


**Figure 2: (a) The modified TrueFISP sequence. (b) The acquired projections with different echo times are spaced by an angle increment of 111.246°**

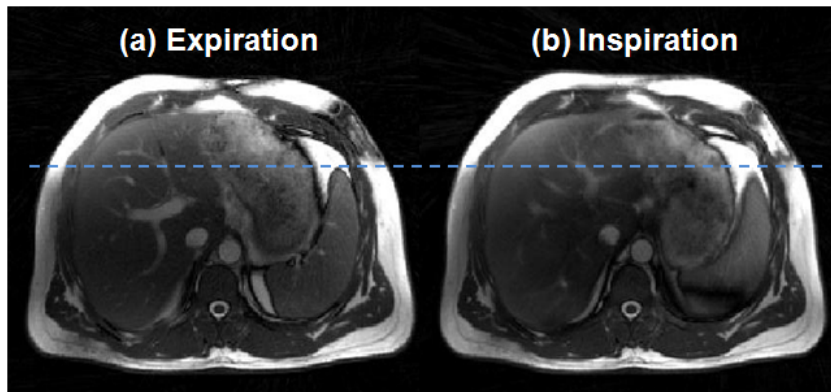


**Figure 3:** Comparison of the two frames reconstructed in different respiratory phases: expiration (a), and inspiration (b)

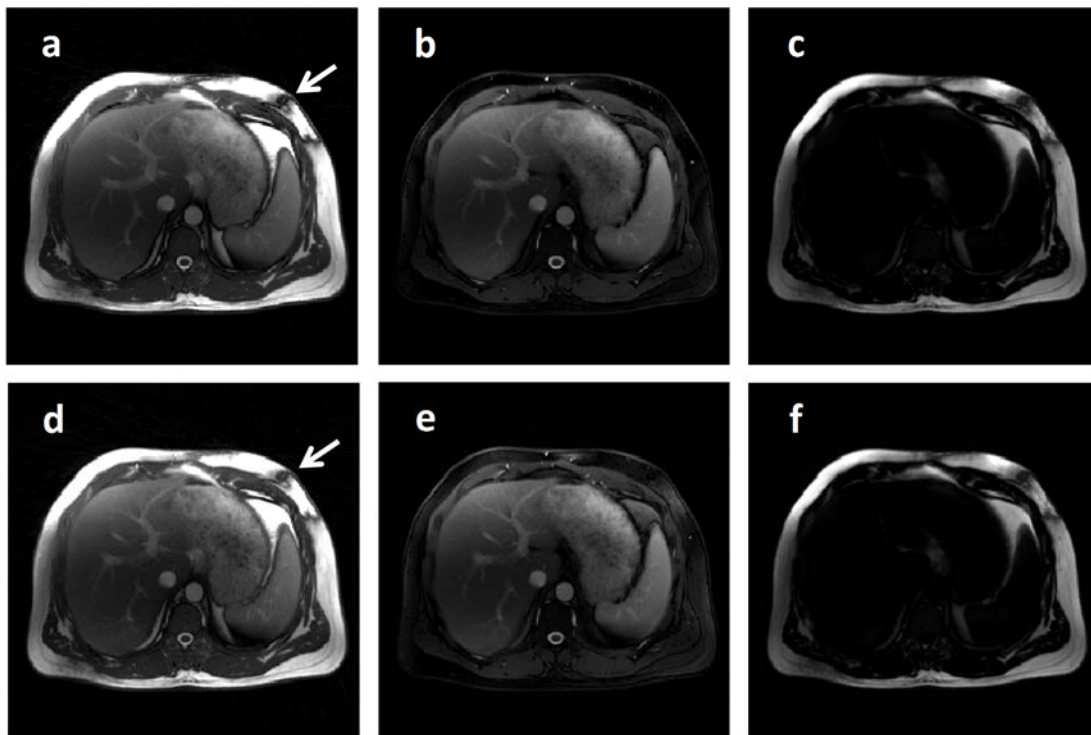


**Figure 4:** Two frames acquired at 3T on healthy volunteer is shown here. (a,d) Unprocessed image. Water-only and fat-only results are shown in (b,e) and (c,f), respectively. The white arrow in (a) indicates banding artifacts

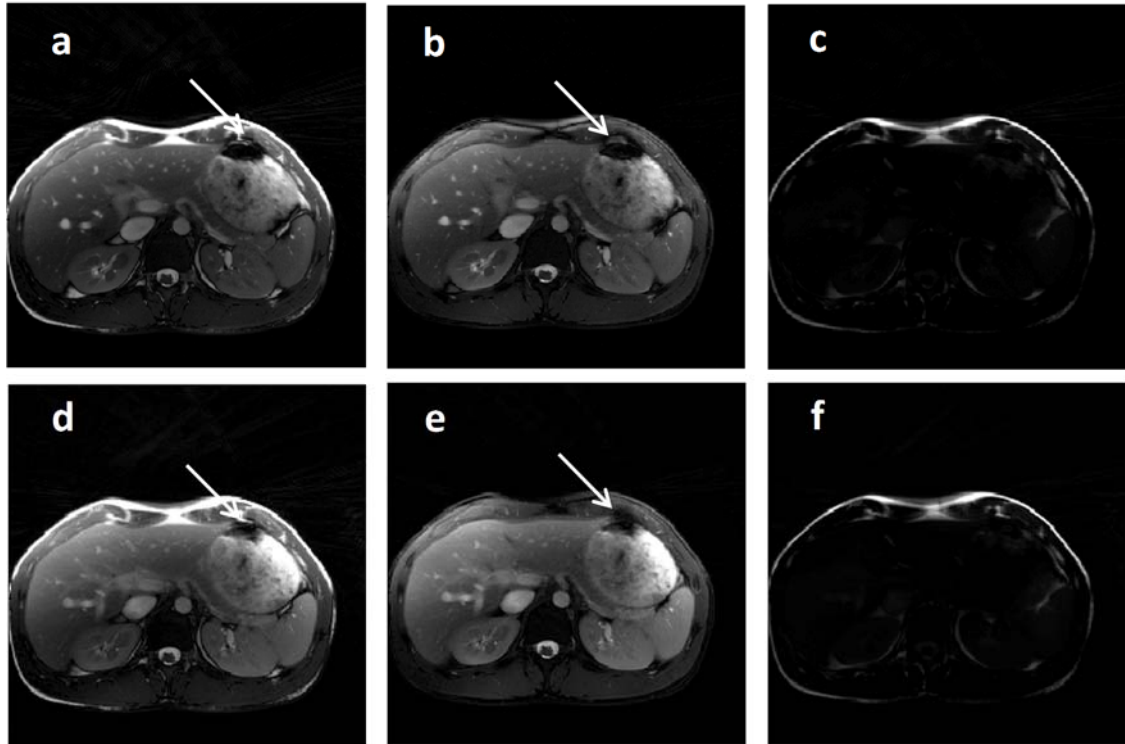


**Figure 5: Two frames for another healthy volunteer is shown here. (a,d) Unprocessed image. Water-only and fat-only results are shown in (b,e) and (c,f), respectively. The white arrow in (a) indicates banding artifacts**

Fig. 3 shows two frames reconstructed in different respiratory phases: expiration (a), and inspiration (b), where the dotted line indicates the variation of the position due to the different respiratory phases. Fig. 4 and Fig. 5 shows the fat and water in healthy volunteers, where the water-only Fig. 4(b,e), Fig. 5(b,e) and fat-only Fig. 4(c,f), Fig. 5(c,f) images were reconstructed using the algorithm proposed in<sup>(13)</sup>, while the unprocessed image is shown in Fig. 4(a,d) and Fig. 5(a,d). Banding artifacts, common with TrueFISP sequences, were observed. The white arrow indicates banding artifacts. A Principal Component Analysis (PCA) was applied to enhance the image quality by reducing the streaking artifacts. These streaking artifacts appear incoherently over the image series due to the quasi-random sampling, the PCA allows

identifying the main feature of the dynamic. Thus, by keeping the principal components with high eigenvalues and throwing away principal components with low eigenvalues, the streaking artifacts are removed while the important features of the dynamic are maintained.

### Discussion

A novel approach to separate fat and water signals in the abdomen combined with KWIC-filtered radial TrueFISP is presented here. The approach provides robust high temporal (~100ms) and high spatial resolution. The separation is achieved by changing the echo time (TE) from projection to projection, to force fat signals to behave in a conspicuous manner over time, in order to be detected and separated from water signals.

The increment  $\Delta TE$  should be large enough to induce large phase differences between the fat and water signals, yet small enough to avoid undue increases in TR in our TrueFISP sequence. A value of  $\Delta TE = 400 \mu s$  was considered an acceptable compromise between these two conflicting demands. The present method could be applicable to clinical applications where good temporal resolution and good fat suppression are both essential; for future work, our approach might prove to be particularly useful for accurate tracking of contrast agent in time under free breathing in fatty tissue. This method is also expected to allow accurate tracking of a contrast agent over time during free breathing.

In this work, the number of KWIC-filtered projections for reconstruction was 631 projections used to reconstruct four images at different TEs and at 21 different time points. The selected number taking into accounts the tradeoff between enhances the image resolution and better SNR. Therefore, despite using a partial part of the acquired data (631 projections out of 2001), but it was sufficient to achieve these goals.

The main magnetic field,  $B_0$ , is not perfectly uniform. The sources of these inhomogeneities include variations in the magnetic field strength that occur near the interface of substances of different magnetic susceptibility, and hardware imperfections. The effect of the magnetic field inhomogeneities (off-resonance) can appear as spatial distortion, signal loss, and/or blurring (the white arrow in Figure 4). The TrueFISP pulse sequence is highly sensitive to off-resonance effects, therefore, it suffers from banding artifacts. These artifacts result whenever off-resonance reaches a value equal to  $\pm 1/2TR$ , which indicates the allowed range

for banding-free imaging. The banding artifact shown in Fig. 4 was generated while using  $TR=4.0$  ms.

The results of our study show that TrueFISP with radial acquisition during free breathing is feasible for abdominal MRI studies and the fat water separation achieved even with small variations in TE (ms) in dynamic objects. Both KWIC and PCA processing enhanced the image quality of the dynamic series. The imaging speed could be enhanced by combined the approach proposed here with other strategies such as partial-Fourier and parallel imaging<sup>(31)</sup>.

### Conclusion

The approach presented here was tested and good separation was obtained without respiratory motion artifacts. The results support the conclusion that a novel approach to separate fat and water signals in the abdomen during free breathing has been developed and implemented here. The fat-water separation for free breathing was achieved by using the modified 2D radial TrueFISP sequence, k-space-weighted image contrast (KWIC) filtering and principal component analysis (PCA). The respiratory motion artifacts have been avoided while continuing to provide high temporal and high spatial resolution. Image streaking artifacts reduced by using both KWIC and PCA method.

**Acknowledgements:** The Deutsche Forschungsgemeinschaft DFG BR 4356/2-1 for funding, and SIEMENS, Healthcare Sector, Erlangen, Germany for technical support.

### References

1. Deshpande VS, Shea SM, Laub G, Simonetti OP, Finn JP, Li D. 3D magnetization-prepared true-FISP: a new technique for imaging coronary arteries. *Magn Reson Med* 2001; 46:494-502.

2. Li D, Paschal CB, Haacke EM, Adler LP. Coronary arteries: three-dimensional MR imaging with fat saturation and magnetization transfer contrast. *Radiology* 1993; 187:401-406.
3. Kayser HW, van der Wall EE, Sivananthan MU, Plein S, Bloomer TN, de Roos A. Diagnosis of arrhythmogenic right ventricular dysplasia: a review. *Radiographics* 2002; 22:639-648.
4. Janaka P, Wansapura. Abdominal fat-water separation with SSFP at 3 Tesla. *Pediatr Radiol* 2007; 37:69-73
5. Dixon WT. Simple proton spectroscopic imaging. *Radiology* 1984; 153:189-194.
6. Glover GH, Schneider E. Three-point Dixon technique for true water/fat decomposition with B<sub>0</sub> inhomogeneity correction. *Magn Reson Med* 1991; 18:371-383.
7. Xiang QS, An L. Water-fat imaging with direct phase encoding. *J Magn Reson Imaging* 1997; 7:1002-1015.
8. Reeder SB, Wen Z, Yu H, et al. Multicoil Dixon chemical species separation with an iterative least-squares estimation method. *Magn Reson Med* 2004; 51:35-45.
9. Hargreaves BA, Vasanaawala SS, Nayak KS, Hu BS, Nishimura DG. Fat-suppressed steady-state free precession imaging using phase detection. *Magn Reson Med* 2003; 50:210-213.
10. Ma J, Slavens Z, Sun W, et al. Linear phase-error correction for improved water and fat separation in dual-echo Dixon techniques. *Magn Reson Med* 2008; 60:1250-1255.
11. Ning BS, Robert JL, Omary RA, and Larson AC; Respiratory Self-Gating for Free-Breathing Abdominal Phase-Contrast Blood Flow Measurements. *J Magn Reson Imaging* 2009; 29:860-868.
12. Tang C, Blatter DD, Parker DL. Accuracy of phase-contrast flow measurements in the presence of partial-volume effects. *J Magn Reson Imaging* 1993; 3:377-385.
13. Ababneh R, Yuan J, Madore. Fat-water separation in dynamic objects using an UNFOLD-like temporal processing. *J Magn Reson Imaging* 2010; 32:962-970.
14. Madore B, Glover GH, Pelc NJ. Unaliasing by Fourier-encoding the overlaps using the temporal dimension (UNFOLD), applied to cardiac imaging and fMRI. *Magn Reson Med* 1999; 42: 813-828.
15. Madore B, Hoge WS, Kwong R. Extension of the UNFOLD method to include free-breathing. *Magn Reson Med* 2006; 55:352-362.
16. Ablitt NA, Gatehouse PD, Firmin DN, Yang GZ. Respiratory reordered UNFOLD perfusion imaging. *J Magn Reson Imaging* 2004; 20:817-825.
17. Lin W, Guo J, Rosen MA, and Song HK. Respiratory motion-compensated radial dynamic contrast-enhanced (DCE)-MRI of chest and abdominal Lesions. *Magn Reson Med* 2008; 60:1135-1146.
18. Song HK, Dougherty L. Dynamic MRI with projection reconstruction and KWIC processing for simultaneous high spatial and temporal resolution. *Magn Reson Med* 2004; 52:815-824.
19. Larson AC, Simonetti OP. Real-time cardiac cine imaging with SPIDER: steady-state projection imaging with dynamic echo-train readout. *Magn Reson Med* 2001; 46:1059-1066.
20. Schaeffter R, Weiss S, Eggers H, Rasche V. Projection reconstruction balanced fast field echo for interactive real-time cardiac imaging. *Magn Reson Med* 2001; 46:1238-1241.
21. Peters DC, Epstein FH, McVeigh ER. Myocardial wall tagging with undersampled projection reconstruction. *Magn Reson Med* 2001; 45: 562-567.
22. Barger AV, Grist RM, Block WF, Mistretta CA. Single breath-hold 3D contrast-enhanced method for assessment of cardiac function. *Magn Reson Med* 2000; 44: 821-824.
23. Glover GH, Pauly JM. Projection reconstruction techniques for reduction of motion effects in MRI. *Magn Reson Med* 1992; 28: 275-289.
24. Altbach MI, Outwater EK, Trouard TP, Krupinski EA, Theilmann RJ, Stopeck AT, Kono M, Gmitro AF. Radial fast spin-echo method for T<sub>2</sub>-weighted MR imaging and T<sub>2</sub> mapping of the liver. *J Magn Reson Imaging* 2002; 16:179-189.
25. Katoh M, Spuentrup E, Buecker A, Manning WJ, Guenther RW, and Botnar RM. MR coronary vessel wall imaging: Comparison between radial and spiral k-space sampling. *J Magn Reson Imaging* 2006; 23:757-762.
26. Trouard TP, Sabharwal Y, Altbach MI, and Gmitro AF. Analysis and comparison of motion-correction techniques in diffusion-weighted imaging. *J Magn Reson Imaging* 1996; 6:925-935.
27. Wei Lin,\* Junyu Guo, Mark A. Rosen, and Hee Kwon Song. Respiratory motion-compensated radial dynamic contrast-enhanced (DCE)-MRI of chest and abdominal lesions. *Magn Reson Med* 2008; 60:1135-1146.
28. Martin J M, Lars KH and Terrence JS. Independent component analysis of functional MRI: what is signal and what is noise?

- Neurobiology 2003; 13:620-629.
29. Samsonov A A, Kholmovski E G, Johnson C R. Determination of the Sampling Density Compensation Function Using a Point Spread Function Modeling Approach and Gridding Approximation. Proc. Intl. Soc. Mag. Reson. Med. 2003; 11.
30. Fessler JA, Sutton BP, Nonuniform fast Fourier transforms using min-max interpolation, IEEE Trans Med Imaging 2003; 51 (2) 560-574.
31. Stabe D, Ritter CO, Breuer, Weng AM, Hahn D and Kostler H. CAIPIRINHA Accelerated SSFP Imaging. Magn Reson Med 2011; 65:157-164.

## الحصول على صور ذات جودة عالية أثناء التنفس الحر عند فصل إشارة الدهون عن إشارة الماء

رياض عبابنة<sup>1</sup>، توماس بنكرت<sup>2</sup>، فيليكس بروير<sup>2</sup>

1- قسم الفيزياء والفيزياء الطبية، جامعة اليرموك، اربد، الأردن.

2- معهد الرنين المغناطيسي، بافاريا، ألمانيا.

### الملخص

**الهدف:** استخدام جهاز الرنين المغناطيسي لفصل إشارة الدهون عن إشارة الماء عند تصوير منطقة البطن أثناء التنفس الحر والحصول على صور ذات جودة عالية من خلال دمج تقنية (KWIC) مع بروتوكول التصوير الشعاعي radial TrueFISP.

**المواد والطرق:** تم استخدام بروتوكول التصوير الشعاعي المسمى radial TrueFISP، بحيث تم تعديله للحصول على زمن إثارة مختلف TE عند كل اسقاط إشعاعي من أجل فصل إشارة الدهون عن إشارة الماء. ومن ثمة تم تطبيق تقنية (KWIC) على الصور التي تم الحصول عليها لتصفيتها من التشوهات وللحصول على صور ذات جودة عالية الجوده. وأخيراً تم إجراء تحليل للصور باستخدام تقنية (PCA) من أجل تقليل الخطوط الظاهرة في الصورة والتي تشوهها وتقلل من جودتها ومن أجل أيضاً زيادة نسبة الإشارة إلى الضوضاء (SNR).

**النتائج:** هنا تم إدماج طريقة فصل إشارة الدهون عن الماء مع تقنية (KWIC)، وتم الحصول على صور ذات جودة عالية لكل من الدهون والماء مع دقة زمنية (~ 100 مللي ثانية) أثناء التنفس الحر.

وتم عرض النتائج مفصلة في هذا البحث.

**الكلمات الدالة:** فصل إشارة الدهون عن إشارة الماء، التصوير الديناميكي، التنفس الحر.